

# Synthesis and properties of phosphorus-containing PEN and PBN copolyesters

Chun Shan Wang\*, Ching Hsuan Lin

Department of Chemical Engineering, National Cheng Kung University, Tainan 701, Taiwan, ROC

Received 3 October 1997; revised 18 December 1997; accepted 7 April 1998

## Abstract

Copolyesters ( $V_a$ – $V_d$  and  $VI_a$ – $VI_d$ ) derived from 2-(6-oxido-6*H*-dibenz(c,e)(1,2)oxaphosphorin-6-yl)-1,4-bis(2-hydroxyethoxy) phenylene (*II*) and bis(2-hydroxyethyl) naphthalate (*III*) or bis(4-hydroxybutyl) naphthalate (*IV*) were synthesized and characterized. Copolyesters  $V_a$ – $V_d$ ,  $VI_a$ – $VI_d$  had been characterized by inherent viscosity, solubilities, t.g.a., d.s.c., X-ray diffraction,  $^1H$  n.m.r.,  $^{31}P$  n.m.r., UL-94 and d.m.a. D.s.c. and X-ray diffraction show that the *VI* series of copolyesters were crystalline polymers and the crystallinity decreased with the increase in *II* content, whereas the *V* series copolyesters were amorphous polymers. The inherent viscosity of these copolyesters ranged from 0.53 to 0.68 dl g<sup>-1</sup>. The  $T_g$  values of the *V* series copolyesters ranged from 118 to 126°C and those of the *VI* series copolyesters were in the range 68–77°C; these were higher than the  $T_g$  values of polyethylene naphthalate (PEN,  $T_g$ : 116°C) and polybutylene naphthalate (PBN,  $T_g$ : 67°C). The  $T_d$  values (10%) for the *V* series of copolyesters in nitrogen ranged from 450 to 470°C and those for the *VI* series copolyesters were in the range 410–415°C; these values were also higher than that of PEN ( $T_d$ : 449°C) and PBN ( $T_d$ : 410°C). UL-94 V-0 grade could be achieved with a phosphorus content as low as 0.48 wt% for the *V* series and 0.97 wt% for the *VI* series copolyesters. T.g.a. kinetics also indicated that the *V* and *VI* series copolyesters had higher activation energies of degradation than did PEN and PBN. When these copolyphosphates were treated with fire for 10 s, intumescence is observed on the surface of copolyphosphates which retards further flaming of the polymers. DMA showed that all copolyphosphate esters have good mechanical properties ( $G'$ : 10<sup>8</sup>–10<sup>9</sup> Pa) before glass transition temperatures. © 1998 Elsevier Science Ltd. All rights reserved.

**Keywords:** Copolyesters; PEN; PBN

## 1. Introduction

Wherever plastics are used in building, construction, electrical equipment, and transportation, flammability is a serious consideration, and it is common to add flame retardants to control it. Of the elements which reduce flammability, organic phosphorus is generally most effective, followed by organic bromide, antimony oxide, and water of hydration. In a fire, bromine, chlorine, and antimony produce problems of smoke, toxicity, and corrosion. Inorganic hydrates must be used in such large amounts that they lower strength properties. Organic phosphates do not cause any of these problems; thus they should be the most desirable class of flame-retardant additives.

In recent years, studies on searching for ways to improve the flame retardancy of polymeric materials have been reported [1–11]. A traditional technique of preparing

flame-retardant polymers is to blend flame-retardant additives with polymeric materials. Bonding flame-retardant groups to polymer backbones, i.e. using a reactive flame retardant, has attracted much attention recently [1–8]. The use of a reactive flame retardant has the advantage of the permanent attachment of the flame retardant. This will lead to a much smaller amount of flame retardant being required to reach a certain degree of flame retardancy. Consequently, there is a much smaller influence on the physical and mechanical properties of the polymers [8,9].

Polyethylene 2,6-naphthalate (PEN) and polybutylene 2,6-naphthalate (PBN) have superior thermal, mechanical, barrier and chemical resistance properties relative to polyethylene 1,4-terephthalate (PET) and polybutylene 1,4-terephthalate (PBT). For this reason, numerous research work is currently under way to develop commercial applications for these new high performance polyesters. However, like other polyesters, the flammabilities of PEN and PBN were a shortcoming in some applications. For improving the flame retardancy and thermal stability, a reactive

\* Corresponding author.

phosphorus-containing diol, 2-(6-oxido-6*H*-dibenz(*c,e*) $\lambda$ (1,2)oxaphosphorin-6-yl)-1,4-bis(4-hydroxyethoxy) phenylene (**II**) was synthesized. Copolyesters with good flame retardancy and thermal stabilities were derived from **II** with bis(2-hydroxyethyl) naphthalate (**III**) or bis(4-hydroxybutyl) naphthalate (**IV**) and characterized in this work. The polymers were characterized by FTIR,  $^1\text{H}$  n.m.r. and  $^{31}\text{P}$  n.m.r. spectroscopy. The thermal stabilities, activation energies of degradation, and flame retardancies were evaluated.

## 2. Experimental

### 2.1. Materials

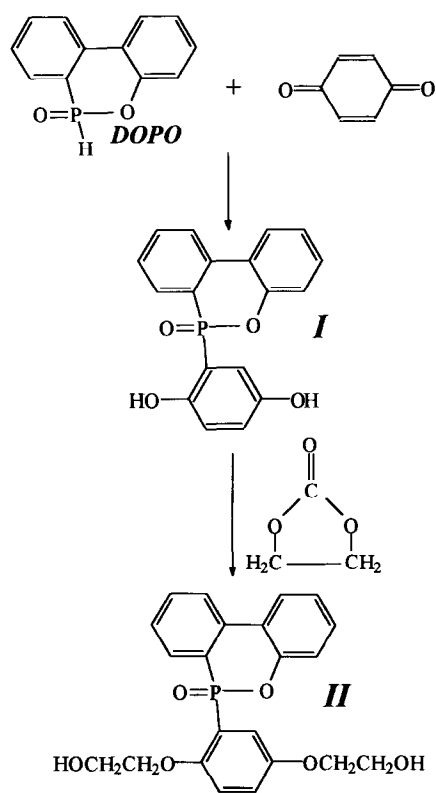
Bis(2-hydroxyethyl) naphthalate (**III**) and bis(4-hydroxybutyl) naphthalate (**IV**) were prepared by ester interchange reaction of ethylene glycol (Ferak) or 1,4-butanediol (Ferak) with 2,6-dimethyl naphthalate (Amoco) respectively [12]. 9,10-Dihydro-9-oxa-10-phosphaphenanthrene-10-oxide - (DOPO) (TCI), 2,6-dimethyl naphthalate (Amoco), ethylene glycol (Ferak), 1,4-butanediol (Ferak), *p*-benzoquinone (Acros), 2-ethoxy ethanol (Acros), potassium iodide (Junsei), ethylene carbonate (Acros) and titanium tetrabutoxide (Merck) were used without further purification. *N,N*-Dimethylacetamide (Acros) was purified by distillation under reduced pressure over calcium hydride (Acros) and stored over 4 Å molecular sieves. Solvents for solubility tests were used without further purification.

### 2.2. Synthesis of 2-(6-oxido-6*H*-dibenz(*c,e*) $\lambda$ (1,2)oxaphosphorin-6-yl)-1,4-dihydroxy phenylene [13] (**I**)

DOPO 1.25 mol, *p*-benzoquinone 1.125 mol and 2-ethoxyethanol 500 g were introduced into a round-bottom 1000 ml glass flask equipped with a nitrogen inlet, a condenser and a mechanical stirrer. The flask was heated to 125°C and maintained at that temperature for 4 h. The reaction product was filtered after cooling to room temperature and washed with 2-ethoxyethanol and methanol. It was further recrystallized from 2-ethoxyethanol and then dried in a vacuum oven at 100°C for 8 h. Off-white crystals (m.p. 255–256°C, 93% yield) of **I** were obtained. Mass (FAB) (*m/e*, relative intensity): 325 ( $M + 1^+$  100), 215 ( $(M - 109)^+$   $\alpha$  cleavage of O=P–Ar, 52). Elemental analysis for  $\text{C}_{18}\text{H}_{13}\text{O}_4$  (324): Calc. (%): C, 66.67; H, 4.04; found (%): C, 66.57; H, 4.10.  $^{31}\text{P}$  n.m.r.: 21.52 (s).

### 2.3. Synthesis of 2-(9,10-dihydro-9-oxa-10-phosphaphenanthrene-10-oxide)-1,4-bis(2-hydroxyethoxy) phenylene (**II**)

2-(6-Oxido-6*H*-dibenz(*c,e*) $\lambda$ (1,2)oxaphosphorin-6-yl)-1,4-dihydroxy phenylene (**I**) 1 mol, ethylene carbonate 3 mol, KI 4 g and DMAc 500 g were introduced into a round-bottom 1000 ml glass flask equipped with a nitrogen inlet,



Scheme 1.

a condenser and a mechanical stirrer. The flask was heated to 160°C and maintained at that temperature for 7 h. The reaction mixture was poured into 1000 ml distilled water which resulted in precipitation of yellow powder. Recrystallization from isopropanol gave yellow crystals (m.p. 157–158°C, 95% yield) of **II**. Mass (FAB) (*m/e*, relative intensity): 413 ( $M + 1^+$  100), 215 ( $(M - 109)^+$   $\alpha$  cleavage of O=P–Ar, 13). Elemental analysis for  $\text{C}_{22}\text{H}_{21}\text{O}_6\text{P}$  (412): Calc. (%): C, 64.02; H, 5.10; found (%): C, 63.99; H, 5.18.  $^{31}\text{P}$  n.m.r.: 19.56 (s).

### 2.4. Synthesis of polymer via melt polymerization

A typical example of the polycondensation is given below and the equation is shown in Scheme 2.

#### 2.4.1. $\text{VI}_d$ from **II** and **IV**

**II** 16.20 g ( $3.93 \times 10^{-2}$  mol), **IV** 90.00 g (0.25 mol),  $\text{Ti}(\text{O}i\text{Bu})_4$  ( $0.3 \times 10^{-4}$  mol) and cobalt(II) acetate tetrahydrate ( $0.3 \times 10^{-4}$  mol) were introduced into a 500 ml three-neck flask fitted with a nitrogen inlet, a mechanical stirrer and a gas outlet connected to a vacuum pump. The reaction mixture was heated to 250–260°C and maintained at that temperature for 80 min. The pressure of the reaction system was gradually reduced to 1–3 mmHg in 60 min. The polycondensation was allowed to proceed at 265°C and 1–3 mmHg for another 60 min. Finally, the pressure was returned to normal atmospheric pressure using nitrogen to prevent degradation by oxidation. A light yellow

copolyester with intrinsic viscosity of  $0.58 \text{ dl g}^{-1}$  measured at a concentration of  $0.5 \text{ g dl}^{-1}$  in tetrachloroethane/phenol (2/3 w/w) solution at  $30^\circ\text{C}$  was obtained. The i.r. (film) spectrum exhibited absorption at  $1178 \text{ cm}^{-1}$  (P–O–Ar),  $1320 \text{ cm}^{-1}$  (P=O),  $1716 \text{ cm}^{-1}$  (C=O),  $2960 \text{ cm}^{-1}$  ( $\text{CH}_2$ ). Chemical shift (ppm) 8.87 (2H of naphthalene in *S* section, s), 8.32 (2H of naphthalene in *S* section, dd), 8.19 (2H of naphthalene in *S* section, dd), 4.92 (4H of  $\text{CH}_2\text{CH}_2\text{CH}_2\text{CH}_2$  in *S* section), 2.46 (4H of  $\text{CH}_2\text{CH}_2\text{CH}_2\text{CH}_2$  in *S* section). The small peaks at 4.17–5.16 (8 aliphatic hydrogens in *R* section), 7.1–8.1 (11 phenylene hydrogens in *R* section) and 8.27–8.94 (6 naphthalene hydrogens in *R* section) correspond to the structure of copolyesters.

### 2.5. Characterization methods

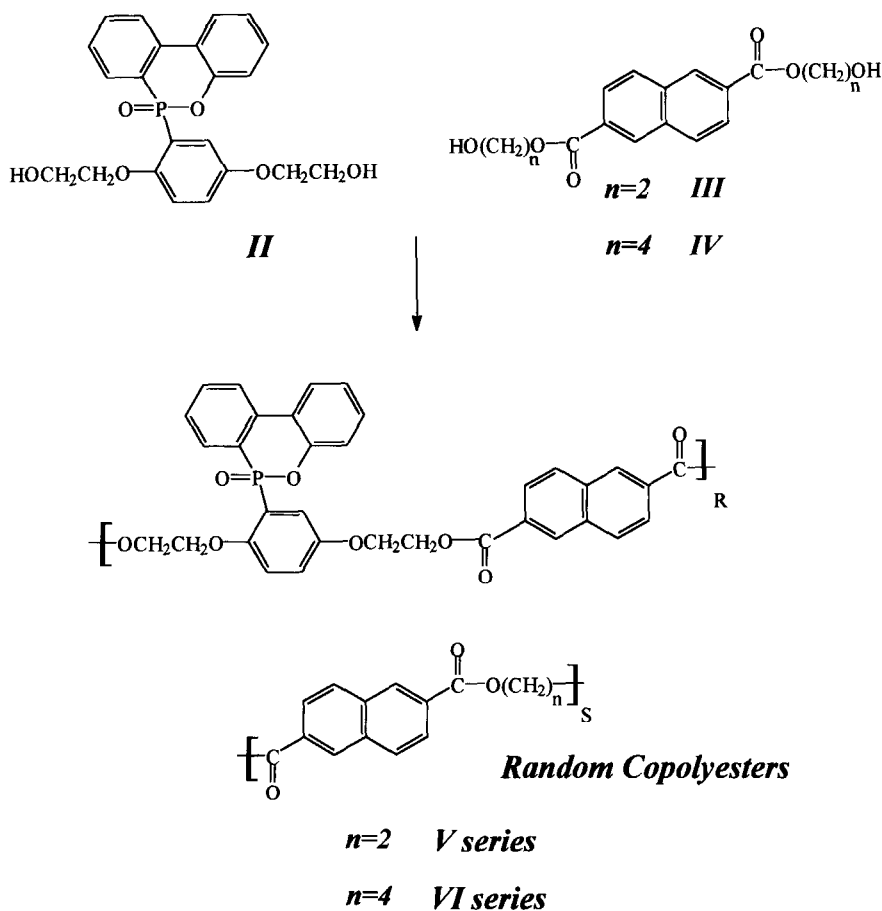
Mass spectra were obtained using a VG 70-250s mass spectrometer. Elemental analyses were performed by the Heraeus CHN-O-Rapid element analyser. Intrinsic viscosities were determined in a tetrachloroethane/phenol (2/3 w/w) solution at  $30^\circ\text{C}$  using an Ubbelohde capillary viscometer (Schott-AVS310). D.s.c. scans were obtained from 3–5 mg samples in a nitrogen atmosphere at a  $20^\circ\text{C min}^{-1}$  heating rate using a Perkin–Elmer DSC 7. Thermal gravimetric analyses were employed with a Perkin–Elmer TGA 7 at a

heating rate of  $20^\circ\text{C min}^{-1}$  in a nitrogen atmosphere from  $30^\circ\text{C}$  to  $800^\circ\text{C}$ . T.g.a. kinetics were employed with heating rates of 10, 20, 30,  $40^\circ\text{C min}^{-1}$  and sample weights of  $5.0 \pm 0.3 \text{ mg}$  were used.  $^1\text{H}$  n.m.r. and  $^{31}\text{P}$  n.m.r. spectra were obtained with a Bruker AMX-400 using *d*-trifluoroacetic acid as a solvent using TMS and  $\text{H}_3\text{PO}_4$  as internal standard respectively. The wide-angle X-ray measurements were performed at room temperature with a Rigaku Geiger Flex D-Max IIIa X-ray diffractometer, using Ni-filtered  $\text{Cu K}\alpha$  radiation. The scanning rate was  $4 \text{ deg min}^{-1}$ . A UL-94V test was performed according to the testing procedure of FMVSS 302/ZSO 3975 with a test specimen bar of 127 mm in length, 12.7 mm in width and up to about a maximum 12.7 mm in thickness. D.m.a. was carried out using a Perkin–Elmer DMA 7 with a  $10^\circ\text{C min}^{-1}$  heating rate at a frequency of 1 Hz. Specimens 10 mm in length, 5 mm in width, and approximately 0.8 mm in thickness were used.

## 3. Results and discussion

### 3.1. Monomer synthesis

*I* was synthesized from DOPO and *p*-benzoquinone



Scheme 2.

(Scheme 1). The disappearance of wavenumber  $2384\text{ cm}^{-1}$  (P–H group in DOPO) and the appearance of wavenumber  $3173\text{ cm}^{-1}$  (board, OH group in *I*) were observed by i.r. Consequently, this addition reaction could be monitored by means of these absorptions. *II* was prepared from *I* and ethylene carbonate by the modified method of Kem et al. [14]. Although faster reaction rates were observed at higher reaction temperatures, the decomposition of the reactant and product was also likely to occur at the high temperature. The preferred operating temperature was  $160\text{--}165^\circ\text{C}$ . The subsidence of carbon dioxide evolution was a convenient indicator for the completion of reaction. In general, about 6–7 h were adequate. A sharp melting point ( $157\text{--}158^\circ\text{C}$ ) of *II* observed by a polarized microscope was a good indication of its high purity. I.r. showed the appearance of wavenumbers  $2928, 2940\text{ cm}^{-1}$  in *II* indicating the  $-\text{CH}_2-$  group was introduced to *II*. The elemental analysis, mass spectrometric analysis, characteristic peaks in the  $^1\text{H}$  n.m.r. and  $^{31}\text{P}$  n.m.r. spectra, and characteristic bands in the i.r. spectrum correlate sufficiently well with the proposed structure.

### 3.2. Synthesis of copolyesters

All of the copolyesters described here were prepared by melt polymerization of the monomers in various molar ratios. Besides the esterification of *II* with *III* or with *IV*, the polycondensation of *III* or *IV* itself could occur at the same time and a copolyester would be generated. The reaction equation is indicated in Scheme 2. To determine the actual composition and phosphorus content of the copolyesters prepared, they were subjected to  $^1\text{H}$  n.m.r. spectroscopy. The results shown in Table 1 reveal that the final phosphorus content was close to that expected. The 2D  $^1\text{H}\text{--}^1\text{H}$  COSY spectrum of *VI<sub>d</sub>* is shown in Fig. 1. Hydrogen atoms at 4.17–5.16 ppm are assigned in Fig. 1. To our surprise, the hydrogen atoms 'a,b' in Fig. 1 were not magnetically equivalent. This may be attributed to the bulky phosphorus-containing side group which hindered the rotation of the C–C bond.

### 3.3. Properties of polymers

The incorporation of the monomer *II* structure into PEN and PBN would also alter their properties; therefore, the glass transition temperature, melting point, solubilities, thermal properties and flame retardancy of the copolyphosphate were studied. As summarized in Table 1, these copolyesters had inherent viscosities of  $0.53\text{--}0.68\text{ dl g}^{-1}$  and their intrinsic viscosities decreased slightly with increasing content of *II*. The solubilities of these polyphosphate esters were tested in various solvents, and the results are summarized in Table 2. PEN and PBN homopolymers had the poorest solubility, and dissolved only partially in *o*-chlorophenol, whereas the solubilities of the copolyesters increased as expected in NMP, *m*-cresol and *o*-chlorophenol on heating. Their enhanced solubilities were attributed mainly to the lack of and reduced crystallinity of the *V* and *VI* series copolyesters respectively. Wide-angle X-ray diffraction patterns shown in Fig. 2 indicate that the *V* series are amorphous. These results may be attributed as follows. (1) There was a substantial difference in angle between the two interring linkages [15]. This could make it more difficult for the repeating unit to fit into a crystal lattice. (2) The mobility of the polymer chain must be one of the important factors governing the crystallinity of copolyesters [15]. A bulky rigid group in the copolyester chain could make it more difficult for this molecule to adopt a configuration that would fit into a lattice structure. (3) Upon cooling of the copolyester, the ester segment may crystallize faster than the ether segment [16]; the ether segments which are located in the amorphous region are restricted in their motion and hence reduce the crystallinity of copolymers. Wide-angle X-ray diffraction patterns for the *VI* series copolyesters shown in Fig. 3 indicated that the *VI* series copolyesters were crystalline polymers. This may be attributed to the flexible and long butylene segment making this molecule adopt a configuration that would fit into a lattice structure easily. The X-ray diffraction patterns showed that the copolyesters had the same lattices as the

Table 1  
The phosphorus content, inherent viscosities and thermal properties of the *V* and *VI* series copolyesters

	Feed (mol/mol) <i>III/IV</i>	<i>P</i> (wt%)		Intrinsic viscosity <sup>a</sup> (dl g <sup>-1</sup> )	<i>T<sub>g</sub></i> (°C)	<i>T<sub>m</sub></i> (°C)	$\Delta H_f$ (J g <sup>-1</sup> )	<i>T<sub>mc</sub></i> (°C)	$\Delta H_c$ (J g <sup>-1</sup> )
		expected	final						
PEN	0/0.35	0	0	0.67	116.2	262	18.34	—	—
<i>V<sub>a</sub></i>	$1.75 \times 10^{-2}/0.35$	0.5	0.48	0.63	119.3	—	—	—	—
<i>V<sub>b</sub></i>	$2.82 \times 10^{-2}/0.35$	1	0.98	0.64	125.3	—	—	—	—
<i>V<sub>c</sub></i>	$4.5 \times 10^{-2}/0.3$	1.5	1.46	0.58	126.8	—	—	—	—
<i>V<sub>d</sub></i>	$6 \times 10^{-2}/0.3$	2.0	1.91	0.57	127.2	—	—	—	—
PBN	0/0.25	0	0	0.68	67.1	241.3	42.1	196.3	35.6
<i>VI<sub>a</sub></i>	$5.60 \times 10^{-3}/0.25$	0.25	0.25	0.64	71.4	237.8	40.3	199.2	34.9
<i>VI<sub>b</sub></i>	$1.15 \times 10^{-2}/0.25$	0.5	0.49	0.60	72.6	233.3	38.0	188.0	33.8
<i>VI<sub>c</sub></i>	$2.45 \times 10^{-2}/0.25$	1.0	0.97	0.58	74.1	225.7	34.9	180.4	31.4
<i>VI<sub>d</sub></i>	$3.93 \times 10^{-2}/0.25$	1.5	1.43	0.53	77.3	216.7	22.8	—	—

$\Delta H_f$ : melting enthalpy; *T<sub>mc</sub>*: melting crystallization temperature;  $\Delta H_c$ : melting crystallization enthalpy

<sup>a</sup> Measured at  $30^\circ\text{C}$  at a concentration of  $0.5\text{ g dl}^{-1}$  in tetrachloroethane/phenol (2/3 w/w)

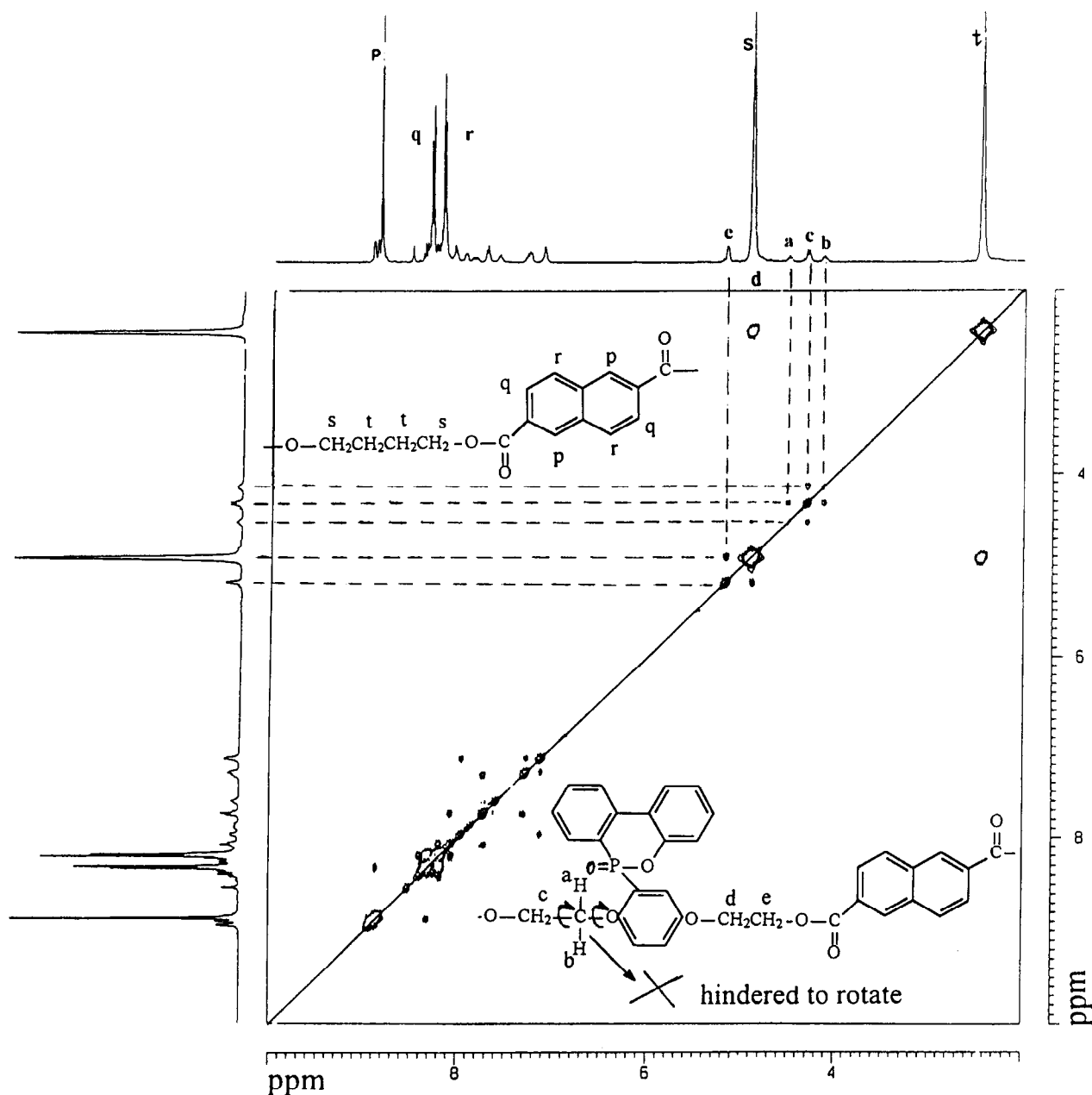


Fig. 1. The  $^1\text{H}$ - $^1\text{H}$  COSY spectrum of  $\text{VI}_d$ .

crystal of PBN. This result indicates that the crystallinity of the  $\text{VI}$  series copolyesters may be attributed to crystallization of PBN segments.

The first d.s.c. scans of the  $\text{VI}$  series and PBN are shown in Fig. 4. The  $T_g$  values of the  $\text{VI}$  series increased slightly with increasing content of  $\text{II}$ . The  $T_g$  values, melting enthalpies  $\Delta H_f$ , melting crystallization temperature  $T_{mc}$  and melting crystallization enthalpies  $\Delta H_c$  are shown in Table 1. The melting enthalpies decreased with increasing  $\text{II}$  content, indicating a reduction in the degree of crystallinity with increasing  $\text{II}$  content. The  $\text{V}$  series of copolyesters showed rather featureless d.s.c. traces from the  $T_g$  values to  $420^\circ\text{C}$ , indicating there were no melting points

for the  $\text{V}$  series copolyesters. This result supported the amorphous pattern in the X-ray diffraction.

The change of melting temperature with copolymer composition was analysed by the Flory equation [17]

$$\frac{1}{T_m} - \frac{1}{T_{m,0}} = -\frac{R}{\Delta H_u} \ln X$$

where  $T_m$  is the melting temperatures of the  $\text{VI}$  series copolymer,  $T_{m,0}$  is the melting temperature of PBN homopolymer,  $X$  is the mole fraction of the crystallization unit ( $\text{IV}$ ), and  $\Delta H_u$  is the heat of fusion of a crystallizable unit.

$T_{m,0}$  may be determined either directly from the pure polymer or by a plot of  $T_m^{-1}$  versus  $-\ln(X)$ . The latter is

Table 2  
Solubilities<sup>a</sup> of V and VI series copolyesters

	DMF	DMAc	NMP	<i>m</i> -Cresol	OCP	ODB	DMSO	THF	Methanol
PEN	—	—	—	—	+h	—	—	—	—
V <sub>a</sub>	—	—	—	—h	+h	+h	—	—	—
V <sub>b</sub>	—	—	—h	—h	+h	+h	—	—	—
V <sub>c</sub>	—	—	—h	—h	+h	+h	—	—	—
V <sub>d</sub>	—	—	+h	+h	+h	+h	—h	—	—
PBN	—	—	—	—	—	—	—	—	—
VI <sub>a</sub>	—	—	—	+h	—	—	—	—	—
VI <sub>b</sub>	—	—	—h	—h	+h	—h	—	—	—
VI <sub>c</sub>	—h	—h	+h	+h	+h	—h	—	—	—
VI <sub>d</sub>	+h	+h	+h	+h	+h	+h	—h	—	—

NMP: *N*-methyl-2-pyrrolidone; DMF: *N,N*-dimethylformamide; DMAc: *N,N*-dimethylacetamide; DMSO: dimethyl sulfoxide; OCP: *o*-chlorophenol; ODB: *o*-dichlorobenzene

<sup>a</sup> Solubility: +h, soluble on heating; —h, partially soluble on heating; —, insoluble on heating

very useful in the case where the polymer decomposes below its melting temperature. In the VI series of copolyesters, the plot of  $T_m^{-1}$  versus  $-\ln(X)$  according to Flory's equation exhibited a good linearity, as shown in Fig. 5. The intercept in Fig. 5 gives a  $T_{m,0}$  value of 241.6°C, very close to the experimental value (241.3°C) of the PBN homopolymer.

T.g.a. traces of phosphorus-containing copolyphosphates provided additional information regarding thermal stability and thermal degradation behaviour. T.g.a. curves of the V and VI series copolyesters in nitrogen are shown in Fig. 6. The 10% degradation temperature ranged from 450 to 470°C and from 410 to 415°C for the V series and the VI series respectively. The char yields at 700°C and the thermal decomposition temperature  $T_d$  of the copolyesters in nitrogen increased slightly with increasing II content. The t.g.a. traces of these copolyphosphates in air (Fig. 7) revealed two decomposition steps because of oxidative degradation of the carbonaceous residue. Their 10% degradation temperature

decreased slightly. Van Krevelen [18] has proposed that the char residue on pyrolysis is linearly proportional to the oxygen index of halogen-free polymers. Compared with PEN, the char yield at 600°C in air for the V series copolyesters improved drastically, so incorporation of monomer II is beneficial to the thermal properties and flame retardancy of PEN and PBN. Fig. 8 shows the isothermal t.g.a. traces of PEN and V<sub>c</sub> at 350°C, 400°C, 450°C. The char yield of V<sub>c</sub> was higher than PEN at each temperature, which was consistent with the results shown in Fig. 7. The surface of V<sub>c</sub> after fire for 10 s is shown in Fig. 9. Intumescence is observed which retards further production of combustible gases, decreases the exothermicity due to pyrolysis reactions, decreases the thermal conductivity of the surface of a burning material and consequently limits the flammability of the materials. In general, the incorporation of a phosphorus linkage into the polymer main chain results in lower thermal stability of polymer [2–5] and their

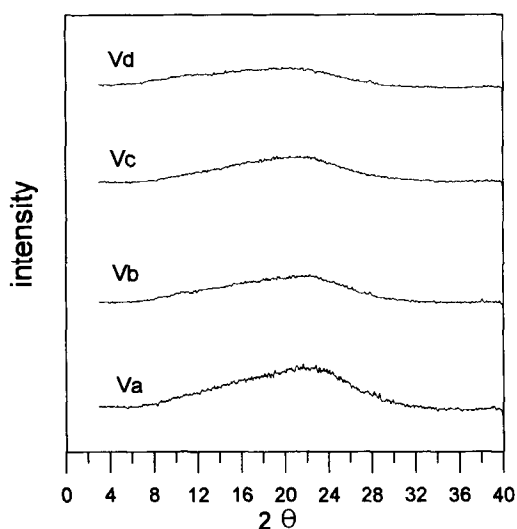


Fig. 2. Wide-angle X-ray diffraction patterns of the V series copolyesters.

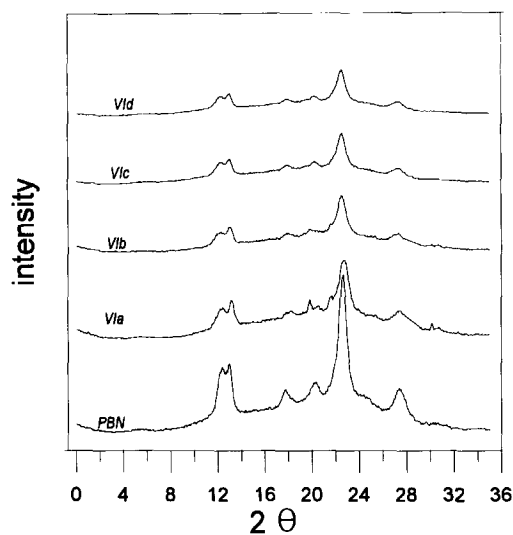


Fig. 3. Wide-angle X-ray diffraction patterns of PBN and the VI series copolyesters.

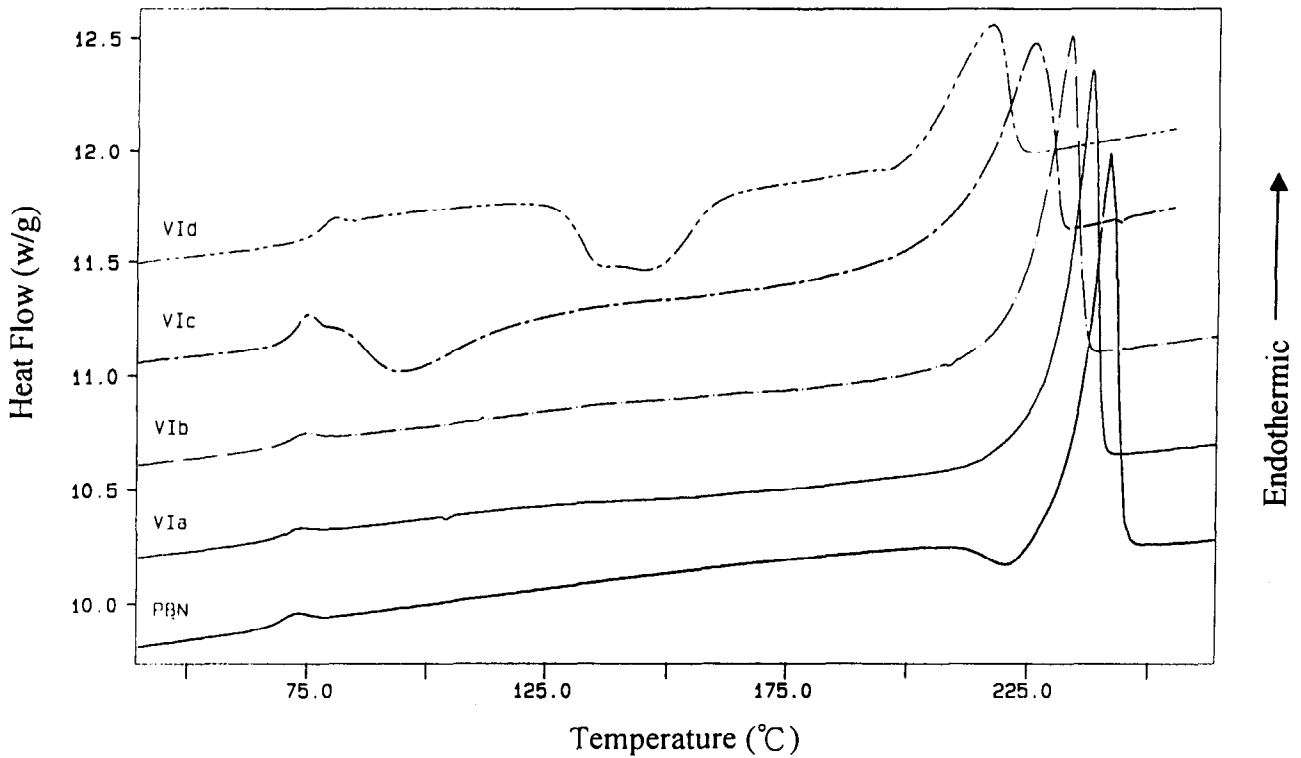


Fig. 4. First d.s.c. scans of the *VI* series copolyesters and PBN.

degradation temperatures were around 200–300°C [2–5], whereas the copolyphosphates investigated in this paper exhibited higher thermal stability and char yield than PEN and PBN. This extraordinary phenomena may be attributed not only to the increase in aromatic content per repeating unit in the macromolecular chain, but also to the unusual high thermal stability of the P–O–C bond in the *V* and *VI* series copolyesters. Wang and Lin [19] have synthesized phosphorus-containing polyarylates derived from 2-(6-oxido-6H-dibenz(c,e)(1,2)oxaphosphorin-6-yl)-

1,4-dihydroxy phenylene as a pendant group and found that the P–O–C chain did not break below 455°C. The reason for the unusual high thermal stability of the P–O–C bond in the *V* and *VI* series copolyesters may be attributed to the O=P–O group being protected by three phenylene groups. After breaking the pendant O=P–O, the char formed by the pendant O=P–O acts as a protective layer for the polymer main chain, so the phosphorus-containing *V* and *VI* series copolyesters are more stable than PEN and PBN respectively. Table 3 shows the results of the UL-94 test. UL-94 V-0 grade could be achieved with a phosphorus content as low as 0.48 wt% for the *V* series and 0.97 wt% for the *VI* series. The results showed that the incorporation of phosphorus into PEN and PBN was helpful to their flame retardancy.

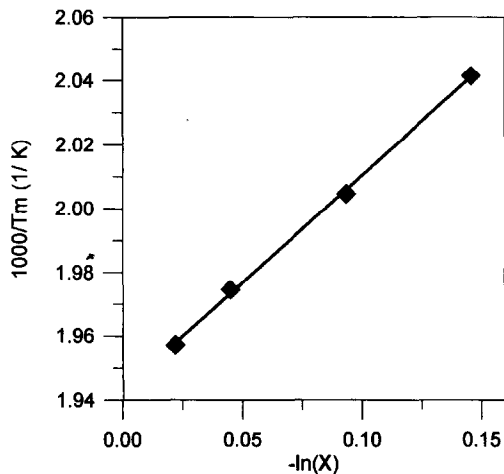


Fig. 5. The plot of  $T_m^{-1}$  versus  $-\ln(X)$  according to Flory's equation.

Table 3  
Results of UL-94 test

Sample	P (%)	Burning time (s)	Fume	Drip	UL-94 classification
<i>V<sub>a</sub></i>	0.48	2	No	No	V-0
<i>V<sub>b</sub></i>	0.98	0	No	No	V-0
<i>V<sub>c</sub></i>	1.46	0	No	No	V-0
<i>V<sub>d</sub></i>	1.91	0	No	No	V-0
<i>VI<sub>a</sub></i>	0.25	7	Yes	Yes	V-1
<i>VI<sub>b</sub></i>	0.49	3	No	Yes	V-1
<i>VI<sub>c</sub></i>	0.97	0	No	No	V-0
<i>VI<sub>d</sub></i>	1.43	0	No	No	V-0

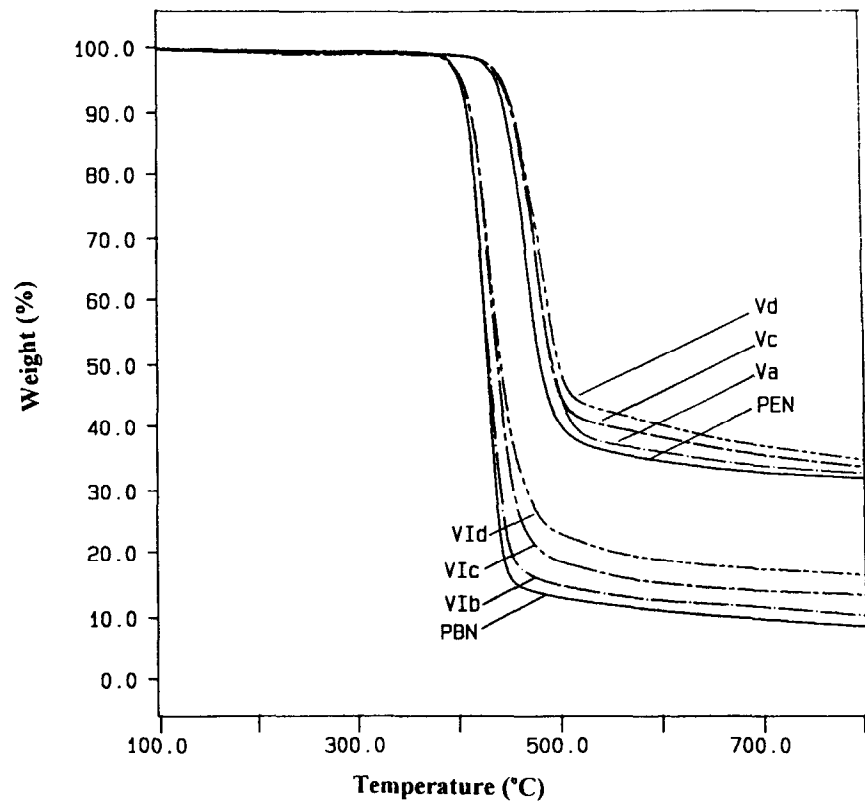


Fig. 6. T.g.a. curves of the V and VI series copolyesters at a heating rate of  $20^{\circ}\text{C min}^{-1}$  in nitrogen.

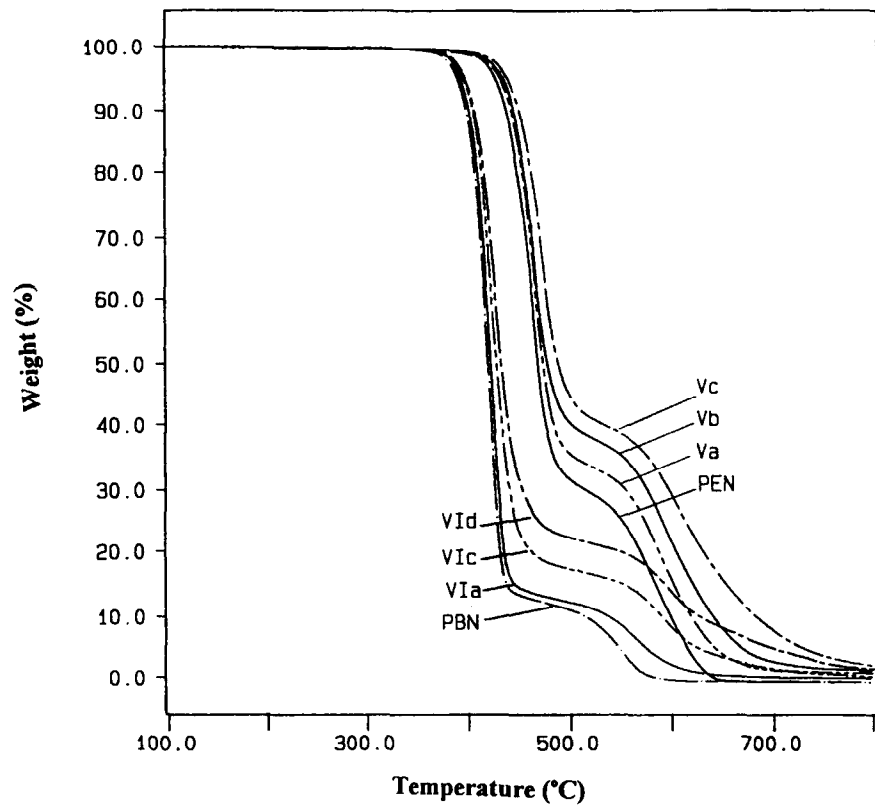


Fig. 7. T.g.a. curves of the V and VI series copolyesters at a heating rate of  $20^{\circ}\text{C min}^{-1}$  in air.

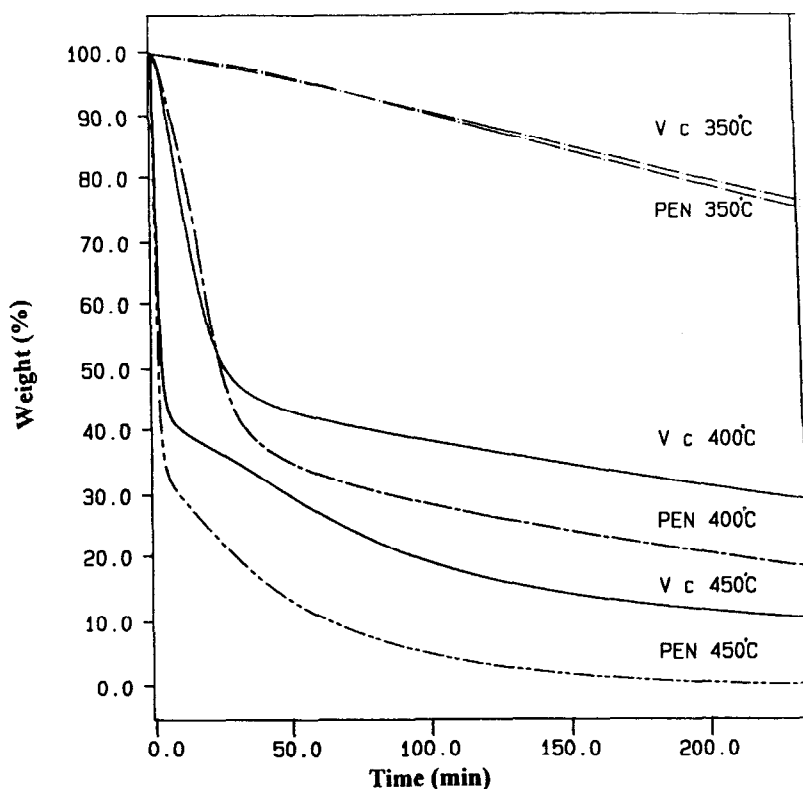


Fig. 8. Isothermal weight loss of the V and VI series copolyesters in air.

The activation energy was determined by Ozawa's method [20] for a given value of weight fraction (wt%). He reported the following equation:

$$\log \beta = \frac{1}{2.303} \ln \beta$$

$$= -0.4567 \frac{E}{RT} + \left[ \log \frac{AE}{R} - \log F(x) - 2.315 \right]$$

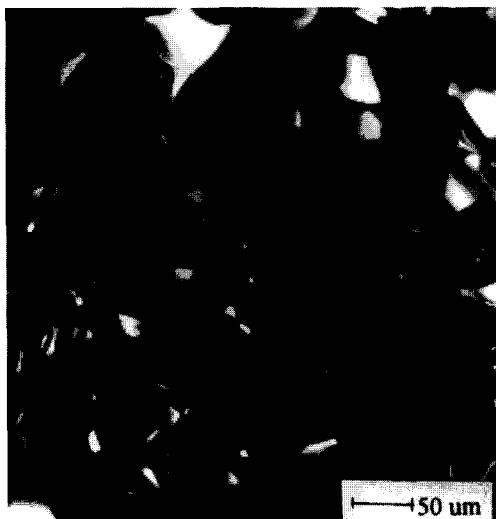


Fig. 9. Surface of  $V_c$  after treating with fire for 10 s.

where  $\beta$  is the heating rate,  $E$  is the activation energy,  $R$  is the ideal gas constant,  $A$  is a pre-exponential factor and  $F(x)$  is a conversion-dependent term.

Thus, at the same conversion, a plot of  $\ln(\beta)$  versus  $T^{-1}$  should be a straight line with a slope of  $(2.303 \times 0.4567)E/R$ . Thus, in dynamic experiments, the activation energy may be obtained as a function of conversion. The results are shown in Fig. 10. Straight lines were drawn according to the method of least squares. From these lines the degradation activation energies of  $V_b$  at various conversions in nitrogen are determined and listed in Table 4. The 20% conversion degradation activation energy of  $V_b$  was  $220.9 \text{ kJ mol}^{-1}$ , which was higher than that of PEN ( $209.2 \text{ kJ mol}^{-1}$ ). Similarly, the 20% conversion degradation activation energy of  $VI_c$  was  $190.4 \text{ kJ mol}^{-1}$ , which was higher than that of PBN ( $187.4 \text{ kJ mol}^{-1}$ ). The results

Table 4

Pre-exponential factors and activation energies of degradation for  $V_b$  at various conversions

Conversion (%)	Pre-exponential factor $\ln A \text{ (s}^{-1}\text{)}$	Activation energy $E \text{ (kJ mol}^{-1}\text{)}$
10	27.8	203.7
20	31.0	220.9
30	31.1	221.1
40	30.8	218.3
50	30.8	217.8

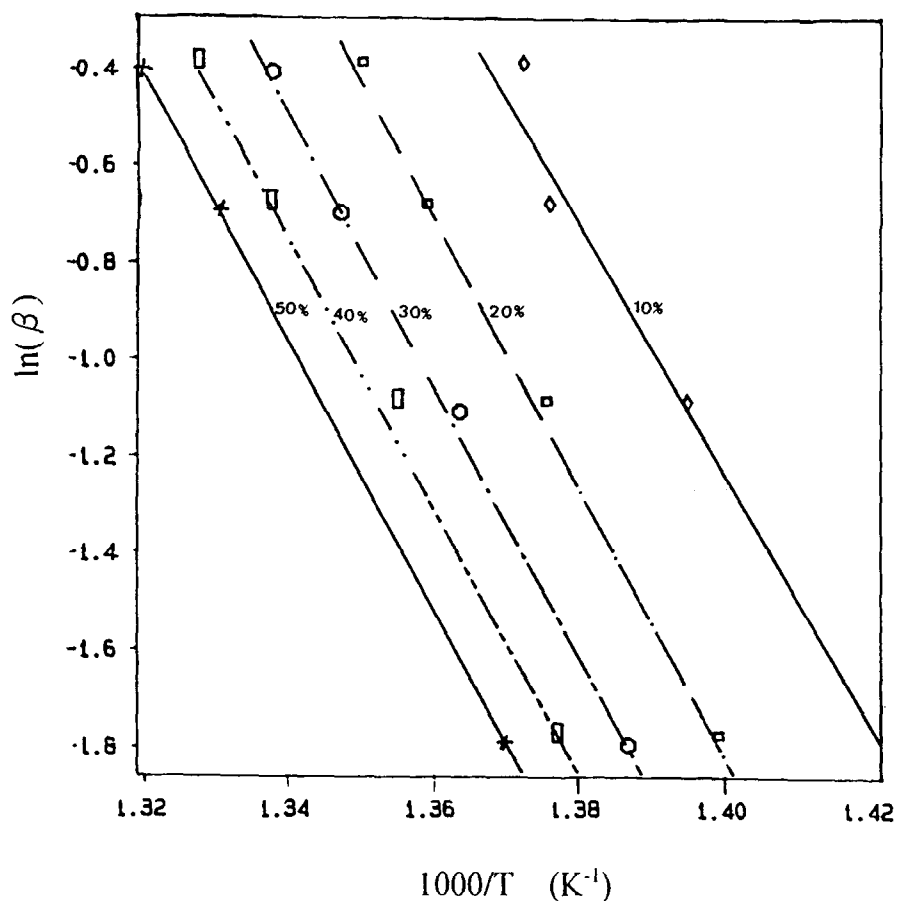


Fig. 10. The plot of  $\ln(\beta)$  versus  $T^{-1}$  for  $V_b$  at various conversions.

in Table 4 indicate that the incorporation of a phosphorus side chain increases the degradation activation energies of PEN and PBN.

Fig. 11 shows the dynamic mechanical analyses curves of

$V_c$  at a heating rate of  $10^\circ\text{C min}^{-1}$  from  $-100$  to  $150^\circ\text{C}$ . The main transition at around  $129^\circ\text{C}$  is associated with approximately a two order of magnitude decrease in  $G'$ . This transition could be indicative of either a glass or a

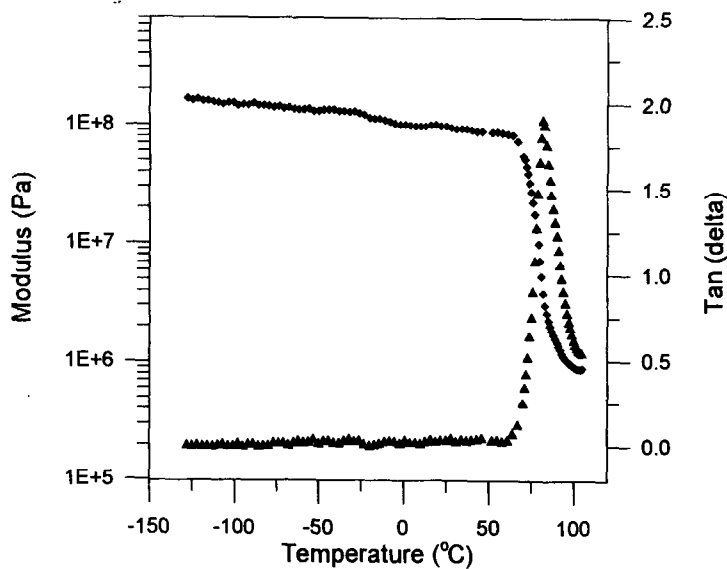


Fig. 11. DMA curves of  $V_c$  at a heating rate of  $10^\circ\text{C min}^{-1}$ .

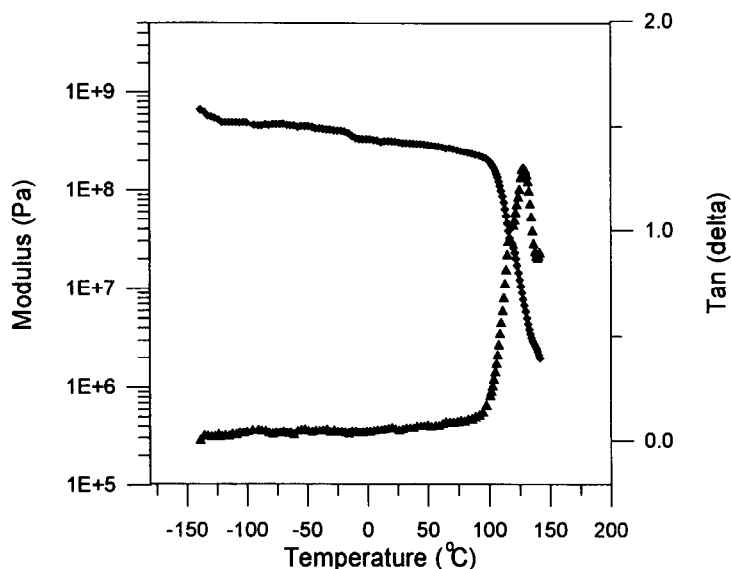


Fig. 12. DMA curves of  $VI_d$  at a heating rate of  $10^\circ\text{C min}^{-1}$ .

melting transition. Moreover, an endothermic transition was observed by d.s.c. at about the same temperature, a fact which supports the glass transition temperature.  $V_c$  exhibited a rather high initial  $G'$  value ( $\sim 10^9$  Pa) and about  $10^8$  Pa up to  $110^\circ\text{C}$ . Fig. 12 shows DMA curves of  $VI_d$  with a main transition at around  $82^\circ\text{C}$ , which is the glass transition temperature of  $VI_d$ . The dynamic mechanical analyses shown in Figs 11 and 12 show no other relaxation (based on  $\tan \delta$ ) except the glass relaxation. This result indicates that the incorporation of a bulky phosphorus-containing side group would not affect (decrease) the mechanical properties before the  $T_g$ . Other  $V$  and  $VI$  series copolyesters showed similar dynamic mechanical behaviour and have good mechanical properties ( $G'$ :  $10^8$ – $10^9$  Pa) by DMA.

#### 4. Conclusions

A series of copolyesters derived from **II** and **III** or **IV** were synthesized successfully by the melt process. These polyphosphate esters have good mechanical properties ( $G'$ :  $10^8$ – $10^9$  Pa) before the glass transition temperature and better thermal ( $T_g$ ,  $T_d$ , char yield) and flame retardant properties than either PEN or PBN. The UL-94 V-0 grade can be achieved with a phosphorus content as low as 0.48 wt% for the  $V$  series and 0.97 wt% for the  $VI$  series. These properties should make the modified PEN or PBN attractive for practical applications such as flame-retardant engineering plastics.

#### Acknowledgements

Financial support of this work by the National Science Council of Republic of China is gratefully appreciated (NSC87-2622-E-006-005).

#### References

- [1] Nair CPR, Glouet G, Brossas J. *J Polym Sci Polym Chem* 1988;26:1791.
- [2] Annakutty KS, Kishore K. *Polymer* 1988;29:756.
- [3] Kishore K, Annakutty KS, Mallick IM. *Polymer* 1988;29:762.
- [4] Annakutty KS, Kishore K. *Polymer* 1988;29:1273.
- [5] Kannan P, Gangadhara, Kishore K. *Polymer* 1909;1991:32.
- [6] Nair CPR, Glouet G, Guilbert Y. *Polym Degrad Stab* 1992;26:305.
- [7] Baillet C, Gandi S, Breant P, Delfosse L. *Polym Degrad Stab* 1992;37:149.
- [8] Banks M, Ebdon JR, Johnson M. *Polymer* 1993;34:4547.
- [9] Banks M, Ebdon JR, Johnson M. *Polymer* 1994;35:3470.
- [10] Banerjee S, Palit SK, Maiti S. *J Polym Sci Polym Chem* 1994;32:219.
- [11] Horrocks AR, Zhang J, Hall ME. *Polym Int* 1994;33:303.
- [12] Wang CS, Sun YM. *J Polym Sci Part A: Polym Chem* 1994;32:1305.
- [13] JP Kokai 5-331179, 1993.
- [14] US Patent 4 261 922, 1981.
- [15] Attwood TE, King T, Leslie VJ, Rose JB. *Polymer* 1977;18:369.
- [16] Boussias CM, Peters RH, Still RH. *J Appl Polym Sci* 1980;25:855.
- [17] Sperling LH. *Introduction to physical polymer science*, 2nd edn. New York: Wiley, 1993:253.
- [18] Van Krevelen DW. *Polymer* 1975;16:615.
- [19] Wang CS, Lin CH, submitted to *Macromolecules*.
- [20] Ozawa T. *Bull Chem Soc Jpn* 1965;38:1881.